THE BEHAVIOR OF PICKWICK LANDING DAM SAND UNDER CYCLIC LOADING

Gogot S. BUDI[1]

ABSTRACT: This paper presents the cyclic load-controlled tests to investigate the liquefaction potential of non-plastic soil samples. The 71 mm diameter samples were trimmed from undisturbed-frozen samples and tested using the MTS servo controlled dynamic testing system. The tests were conducted at the effective confining pressures (σ'_3) of 107 kPa (1 tsf) and 321 kPa (3 tsf) with the frequency of 1 Hz. The results show that the almost all samples reach a zero effective strength condition ($\sigma' \approx 0$) at the cyclic strains between 0.5% and 4%. The relation between number of cycles, to generate 1% cyclic strain, and the stress ratio is linear. The tendency of pore pressure buildup at 1% cyclic strain decreases with the increase of stress ratio.

KEYWORDS: sand, cyclic, liquefaction, triaxial

1. INTRODUCTION

The earthquake zones in the USA, that divides the country into several zones based on earthquake magnitudes, has recently remapped. As a result, the new earthquake zone changes some areas from lower level to higher level of intensity and vise versa. Concerning to the greater risk from an earthquake disaster, few structures that suspected would not survive under strong ground shaking and create devastating impact to human life were reviewed.

The states of Kentucky and Tennessee have several man-made earth dams along Mississippi river that susceptible to a ground movement. Realizing the devastating disaster to human life would occur if the dams fail under ground excitation, the government of both states assigned Harza Engineering consultant, based in Chicago, to investigate the performance of its earth dams subjected to earthquake loading. Since the dams were constructed using non-plastic materials, the investigation was focused on determining their liquefaction potential.

The laboratory tests, which include moisture content, fine content determination, and cyclic triaxial loading to simulate earthquake excitation, were performed at the Geotechnical Engineering Laboratory of Illinois Institute of Technology at Chicago-USA.

2. SAMPLING AND STORING OF SAMPLES

The geological formation of the Pickwick landing dams is dominated by non- cohesive soils that, in natural conditions, is possible to get “undisturbed” samples. Special method is required to obtain undisturbed samples of this formation, since the soil is very sensitive to disturbance due to the lack of

[1] *Lecturer, Department of Civil Engineering, Petra Christian University, Surabaya*

bonding among soil particles. In this project, freezing method was applied prior to the sub-surface exploration.

The general procedure of sampling method can be explained as follows. First of all, the liquid-Nitrogen was injected into the ground at a certain depth, where samples of soil would be explored, to freeze the soil around the tip of the injection pipe. When the bulb of ice was large enough to be cored, then, the sampling process was performed. The samples were stored in the cold storage as soon as possible to avoid melting, and shipped to the laboratory. A cold storage box (freezer) was used to store frozen soil samples in the Laboratory. All samples were trimmed and prepared in room temperature. The dimension of all samples was 71mm in diameter and its lengths were about 140mm.

The remains of the trimmings were collected and used to determine its moisture content (w_c) and fine content (passing sieve # 200). To calculate the void ratio, the specific gravity (Gs) of all samples was assumed 2.70. This value was based on the previous average data determined for one-way triaxial cyclic loading tests [1].

3. TRIAXIAL TESTING PROGRAM

All samples were tested using the MTS servo controlled dynamic testing system at the geotechnical engineering laboratory of Illinois Institute of Technology. To simulate earthquake loading, a two-way cyclic loading was applied to all samples at the frequency of 1 cycle per second (1Hz). The two-way terminology was used to define the type of loading application, where the sample was sheared cyclically in compression and extension (not to be confused with tension).

A set of data acquisition was set up to collect and record all data, which were generated from the machine during the test. This information, which includes pore water pressure, displacement (or strain), and the magnitude of loading (stress), was recorded as many as 20 readings per second. All samples were saturated by applying back- pressure, so that its degree of saturation (which was defined as B value) was more than 96%. The samples, then, were consolidated isotropically under effective confining stress of 107 kPa (1 tsf) or 321 kPa (3 tsf).

The amplitude of cyclic shearing stress (σ_d) was applied based on the given stress ratio (SR), which was defined as the ratio between the applied pressure and 2 times the effective confining stress $\sigma_d/2\sigma'_3$, varied from 0.14 to 0.27 and from 0.24 to 0.38 for samples with confining pressure of 321 kN/m^2 and 107 kN/m^2, respectively.

All samples were sheared under stress-controlled condition, where the stress (load) application was constant during the test, and started by compression stress, as illustrated in Figure 1 (the cyclic loading for Sample US4912). The test was terminated when the sample has reached the zero effective stress condition ($\sigma' = 0$), the state where pore pressure buildup in the sample was equal to the effective confining pressure (σ'_3), or when the excessive deformation has occurred. The characteristics of the samples and the testing program are tabulated in Table 1.

Table 1. The samples characteristics and the testing program

No.	Sample Number	Unit Weight (ton/m^3)		Water Content (w_c)	Void Ratio (e)	Fine (%)	Eff.Conf. Pressure (kPa)	SR $\sigma'_d / 2\sigma'_3$
		γ	γ_d					
1	US5511	2.00	1.62	23.87	0.68	50	107	0.30
2	US5512	2.00	1.62	23.48	0.67	65	321	0.27
3	US5331	1.93	1.53	26.15	0.78	67	107	0.35
4	US5341	1.96	1.60	22.97	0.70	67	321	0.23
5	US4912	1.96	1.62	21.54	0.67	31	107	0.24

6	US4932	1.94	1.54	25.36	0.75	20	321	0.14
7	US4931	1.91	1.53	24.24	0.76	17	107	0.31
8	US4913	1.96	1.62	21.27	0.67	31	321	0.19
9	US5911	1.92	1.56	23.05	0.73	31	107	0.38
10	US5912	1.93	1.59	21.03	0.70	26	321	0.15
11	US5913	2.04	1.72	18.54	0.58	38	107	0.32
12	US6041	2.01	1.70	18.25	0.59	33	321	0.22

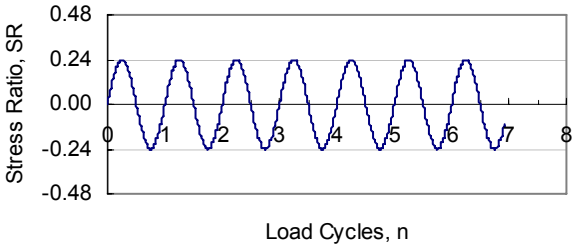

Figure 1. Cyclic load for sample US4912

4. TEST RESULTS

There are two shapes of strain generated from the tests; they were trumpet-like shape and cone-like shape. The first shape formed on the samples when they were sheared cyclically under low Stress Ratio. The axial deformation of the sample was practically constant for the first period of time (or number of cycles), and then grew larger in short period of time (suddenly). The pore water pressure buildup kept increasing from the beginning of the loading application, then followed by sudden jump to about its effective confining pressure so that a $\sigma' = 0$ condition has reached. This state is called liquefaction. In other words, the sample has no shear resistance against loading so that a very large displacement occurred. This type of failure occurred to the samples US4912 and US4932. The pore pressure development and its corresponding strain for these samples are illustrated in Figure 2 and Figure 3. The complete results can be seen in the Report by Budiman and Budi [1].

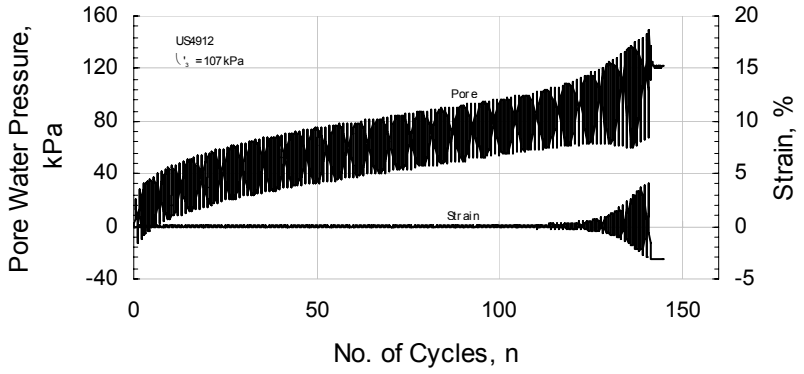

Figure 2. Strain and pore water pressure development of sample US4912

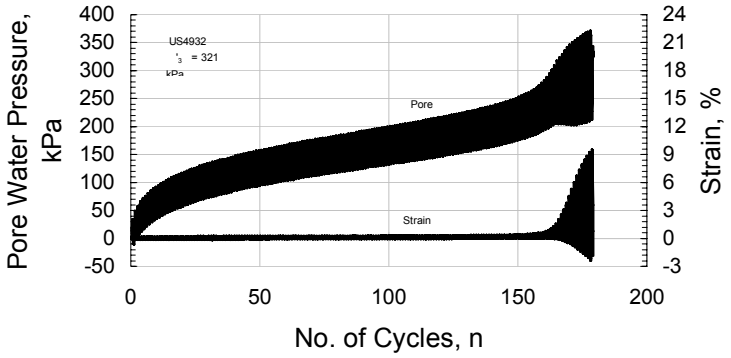

Figure 3. Strain and pore water pressure development of sample US4932

The second shape of strain formed by relatively constant rate of displacement (constant slope) from the beginning of the test and then followed by the sudden increase of displacement. There was no significant increase of pore pressure when the liquefaction occurred. Samples that have this type of shape include US4931 and US5913. The pore pressure development and its corresponding strain for these samples are represented by Figure 4 and Figure 5 for samples US5931 and US5913, respectively.

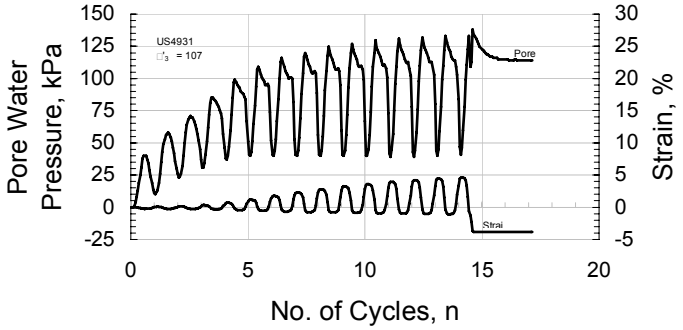

Figure 4. Strain and pore water pressure development of sample US4931

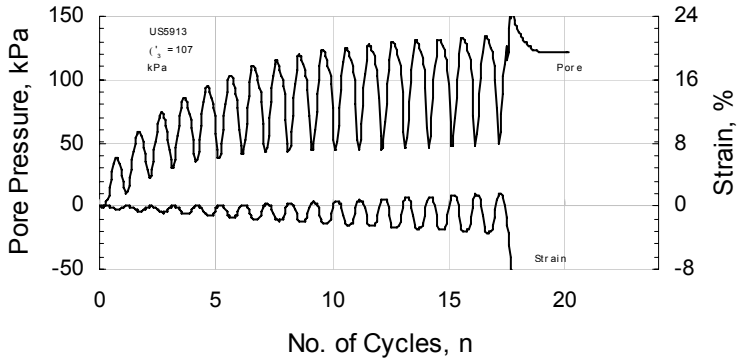

Figure 5. Strain and pore water pressure development of sample US5913

Figure 6 shows the development of strain and pore water pressure under higher shearing stress amplitude (SR = 0.38). The development of pore pressure and strain is almost linear with the number of cycle. The sample failed in less than 4 seconds (4 cycles)

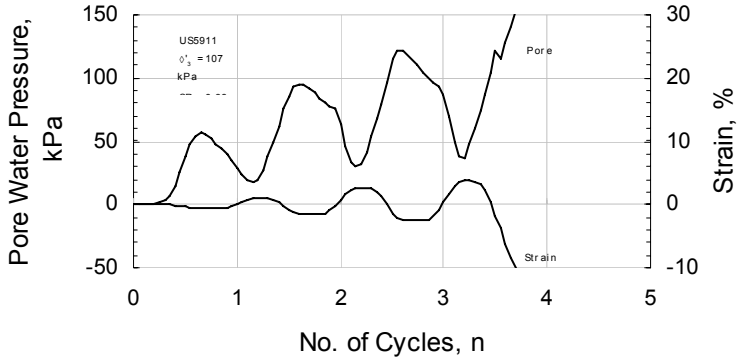

Figure 6. Strain and pore water pressure development of sample US5911

The typical relationship between the deviatoric stress (which is constant for stress-controlled condition) and the total strain can be seen in Figure 7. This figure shows that the displacement in compression is larger than that in extension.

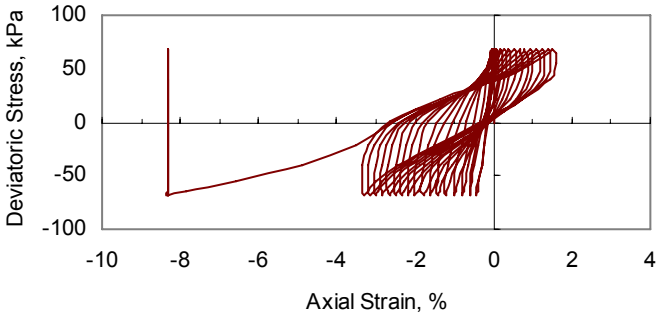

Figure 7. Stress-strain relationship of sample US5913

By normalizing the pore pressure development with its effective confining pressure, the liquefaction of samples confined under effective stress of 107 kPa occurred at the strain of 0.5% to 4%, as shown in Figure 8. Under higher effective confinement (σ'_3 = 321 kPa), three samples have reached the state of zero effective stress at about 0.5% strain, while two of them were considered failed without reaching the state of zero effective strength. The latter phenomenon is illustrated in Figure 9.

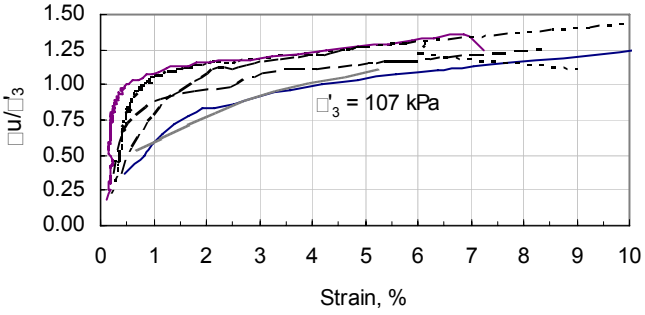

Figure 8. Relationship between normalized pore pressure and strain of samples under effective confining pressure of 107 kPa

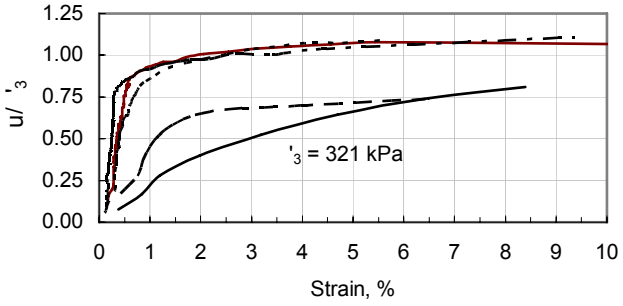

Figure 9. Relationship between normalized pore pressure and strain of samples under effective confining pressure of 321 kPa

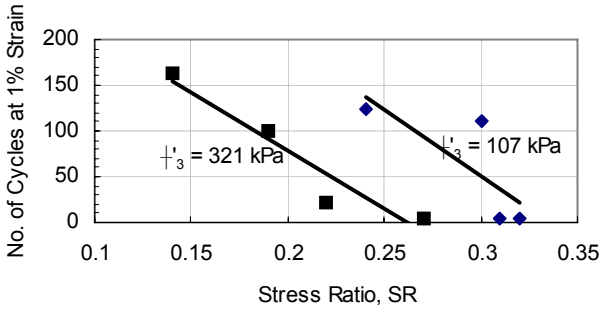

Figure 10. The relationships between stress ratio and no. of load cycles to generate axial cyclic strain of 1%

The relationship between stress ratio and number of loading application to generate liquefaction for samples confined by effective pressure of 107 kPa and 321 kPa is presented in Figure 10. The graph is drawn based upon the assumption that the samples reach liquefaction at the cyclic strain of 1%. This figure shows that the higher the stress ratio the lower number of loading cycles needed to reach liquefaction. It is noticed that the relationship between stress ratio and number of cycles is linear.

Figure 11 shows the relation between maximum and minimum pore pressure buildup and stress ratio at 1% axial strain. The maximum pore pressure relates to the compression loading, while the minimum pore pressure corresponds to the minimum cyclic loading (extension). It is noticed that the

development of pore pressure, at both effective confining pressures, has tendency to decrease with the increase of stress ratio. This phenomenon shows that, under higher cyclic stress amplitude, the rate of strain increment is faster than that of pore pressure development.

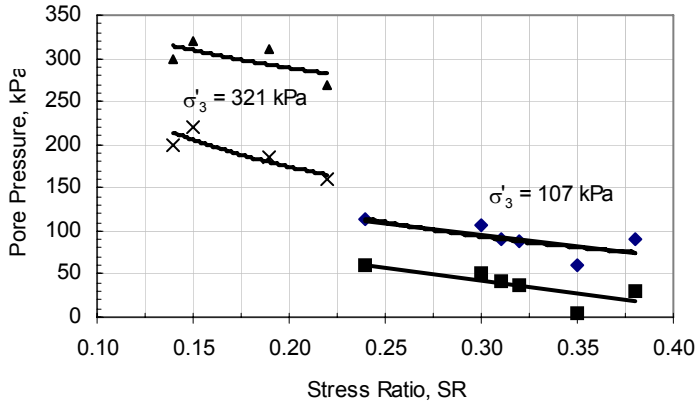

Figure 11. The relationship between pore pressure development and stress ratio

5. CONCLUSION

Based on the analyses of all data collected from this experiment, several conclusions can be underlined.

1. The non-cohesive samples subjected to cyclic loading reach a zero effective strength condition ($\sigma' \approx 0$).
2. The liquefaction occurs at the cyclic strains ranging from 0.5% to 4%.
3. The relation between number of cycles to generate 1% cyclic strain and the stress ratio is linear, and the tendency of pore pressure buildup at 1% cyclic strain decreases with the increase of stress ratio.
4. It is noticed that the development of pore pressure, at both effective confining pressures, has tendency to decrease with the increase of stress ratio

6. REFERENCES

1. Budiman, J. and Budi, G. "*The Behavior of Pickwick Landing Dam Samples and Lexington Dam Samples Under Dynamic Loading"*, Research Report, Department of Civil and Architectural Engineering, Illinois Institute of Technology, Chicago, IL. 60616, 1992.